Desalination and Water Treatment
www.deswater.com
doi: 10.1080/19443994.2013.807049

52 (2014) 1792–1803
February

Taylor & Francis
Taylor & Francis Group

Influence of operating conditions on the retention of phenol in water by reverse osmosis SG membrane characterized using Speigler–Kedem model

Dorra Tabassi*, Amine Mnif, Béchir Hamrouni

Desalination and Water Treatment Research Unit, Faculty of Science of Tunis, University of Tunis El Manar, 2092 manar II, Tunisia
Tel./Fax: + 216 71 871 282; email: dorratabassi@yahoo.fr

Received 26 March 2012; Accepted 5 May 2013

ABSTRACT

Phenol is one of the most common organic water pollutants and strict standards were imposed for phenol content in water because of their high toxicity. Technologies using membrane processes such as reverse osmosis (RO) are increasingly employed in many industrial sectors as important alternative technologies to classical processes of separation. In this work, the removal of phenol from aqueous solutions was studied on laboratory scale by using a commercial polyamide thin film composite RO membranes spiral wound (SG 2514TF by Osmonics Company). The first objective of this work is to evaluate the characteristics of the SG membrane used in permeation experiments with aqueous solution of charged inorganic solutes. A model inspired by the phenomenological approach proposed by Speigler–Kedem was applied in order to quantify separately both parts of mass transfer occurring, the pure convection and the pure diffusion. The experimental results indicated that the retention sequence was inversely proportional to the salt diffusion coefficients in water. The next objective was to study the retention of phenol by SG. Results show that the retention of phenol by SG membrane exceeds 80%. The effect of the chemical parameters (feed concentration, ionic strength, and pH) and the physical parameters (feed pressure and recovery) was studied.

Keywords: Reverse osmosis; Phenol removal; Speigler–Kedem model; Mass transfer

1. Introduction

Now days, water treatment is one of the main important fields of studies due to the increase in the world population and industrial activities. Most of the industries generate a variety of molecules that may pollute waters due to negative impacts for ecosystems and humans (toxicity, carcinogenic, and mutagenic properties). Phenols are chemical products commonly found in various aqueous industrial wastes and they are among the most prevalent forms of chemical pollutants in the industrial wastewater [1,2]. They exist in different concentrations in wastewaters disposed from many industrial processes, including oil refineries,

*Corresponding author.

Presented at the Third Maghreb Conference on Desalination and Water Treatment (CMTDE 2011) Hammamet, Tunisia, 18–22 December 2011

petrochemical plants, ceramic plants, coal conversion processes, phenolic resin industries, and pharmaceutical industries [3,4]. Indentified among priority pollutant by the agency for toxic substances and disease registry, phenol is reported to be associated with intense acute and chronic toxic effect on human health (headache, vomiting, liver and kidney damage, fainting, and other mental disorders) [5]. According to the recommendation of World Health Organization, the permissible concentration of phenolics contents in potable water is $1\,\mu g.\,L^{-1}$ and the regulations by the environmental protection agency call for lowering phenol content in wastewaters less than $1\,mg.\,L^{-1}$ [6,7]. In recent years, interest has been focused on the removal of phenols from aqueous solutions. The conventional techniques such as solvent extraction, adsorption [8,9], chemical oxidation [10,11], UV oxidation, and biological treatment [12] are the most widely used methods for removing and degradation of phenolic compounds in wastewaters. However, these techniques have their own disadvantages such as high-energy consumption, high cost, low efficiency, and secondary pollution [11].

Recently, membrane separation systems have become the important wastewater treatment technologies, facilitating the removal of pollutants and the recovery of solvent, that is, water [13]. For removal of organic pollutants, the application of pressure-driven membrane processes for the removal of low molecular weight organic compounds from wastewater has been analyzed in several recent publications [13–15]. Among membrane-based separation process, the use of reverse osmosis (RO) membrane received growing attention for removal of organic compounds.

The potential of RO processes to remove organic contaminants was first demonstrated by Chian et al. [16]. A number of studies [17–20] have been reported on the use of RO for the removal of organics such as endocrine disrupting chemicals, plastics additives, pesticides, pharmaceutically active compounds, benzene, and toluene. The membrane process utilizing RO membranes have long been an attractive objective in removing of aromatics like phenol [13,21,22]. Various studies have reported that the rejection of organic compound by membranes depends upon both physicochemical properties of solute (acidity, polarity, solute radius) and membrane properties (pore size, charge, and hydrphobicity) [23,24]. Also, the influence of various operating parameters like pressure, feed concentration has been also examined [20,21].

Numerous types of model have been developed to represent solute permeation through RO membrane. Models based on irreversible thermodynamics generally give good results but do not inform on transport mechanisms. Pore flow models were shown to be inappropriate for dense membrane used in the RO process. Solution-diffusion model is widely used because of its simplicity [25].

The polyamide thin film composite RO membrane denoted SG2514TF is used in the study. This membrane offered advantages over traditional cellulose acetate (CA) RO membranes. The most important of these advantages was better rejection of dissolved solids and organics, increased productivity at lower operating pressures, great structural stability and the ability to produce two to three times more purified water per unit area than CA membranes [26].

In the present study, recovery of phenol using SG 2514 TF RO membrane would be investigated. This work deals with the determination of membrane permeability to ultrapure water, the nature of separation mechanism and the molecular weight cutoff. Then, the effects of transmembrane pressure, feed concentration, solution pH, recovery rate, ionic strength on permeate flux and phenol retention would also be studied. The Spiegler–Kedem model was used to calculate the phenomenological parameters, that is, the reflection coefficient ($\bar{\sigma}$) and the solute permeability (P_s) of the membrane to the aqueous solution. The convective and diffusive parts of the mass transfer were quantified.

2. Theory

2.1. Spiegler–Kedem model

The transport of solutes through the membrane pores can be described by using the principles of irreversible thermodynamics where the membrane is considered as a black box. The Spiegler–Kedem [27] model permits to establish a correlation between the permeate flux (J_v) and the solute flux (J_s). For a two components system (solute and solvent), the two basic equations can be written:

$$J_v = L_p(\Delta - \sigma\Delta\pi) \tag{1}$$

$$J_s = P_s(C_0 - C_p) + (1 - \sigma)J_v C_m \tag{2}$$

where C_0, $C_{P,}$ and C_m represent the concentrations of solute in the initial effluent, in permeate and in the membrane, respectively. P_S and σ represent the permeability of solute and reflection coefficient of the membrane, respectively. L_P represents the hydraulic permeability.

ΔP and $\Delta\pi$ represent the transmembrane pressure and the difference in osmotic pressure on both sides

of the membrane. The term ($\sigma.\Delta\pi$) is defined as the critical pressure (P_c).

As can be seen in Eq. (2), the total flux of solute appears as the sum of diffusion and convection terms [28]. Thus, it is possible to write the following equation:

$$J_s = J_{diff} + J_v \cdot C_{conv} = C_p J_v \quad (3)$$

In this expression, J_{diff} represents the permeate flux rate of solute transferred by diffusion (causes by a concentration difference on both sides of the membrane) and C_{conv} represents the concentration of solute in the permeate owing to mass transfer by convection (takes places because of an applied pressure gradient across the membrane). To modulate the selectivity of the membrane toward the solutes, it is possible to favor one or the other mechanism by varying the operating parameters. Some physical parameters such as pressure, tangential flow rate, etc., can greatly influence the mass transfer by convection, whereas some parameters such as complexation, concentration, etc., can influence the mass transfer by diffusion.

The above equation can be rearranged as:

$$C_p = \frac{J_{diff}}{J_v} + C_{conv} \quad (4)$$

Note that this equation is identical to that proposed by Kedem–Katchelsky model [29,30]. The terms J_{diff} and C_{conv} can be determined by plotting the concentration of solute in the permeate (C_P) against the inverse of the permeate flux ($1/J_V$). The function $C_P = f(1/J_V)$ must be a straight line curve whose slope allows to determine J_{diff} and a line whose intercept determine the C_{conv}. Indeed, from the values of (C_{conv}), it is possible to determine the molecular weight cutoff (MWCO) of the membrane with a given salt using the following equation [31]:

$$C_{conv} = C_0\left[1 - (M/\mathrm{MWCO})^{\frac{1}{3}}\right]^2 \quad (5)$$

where M represents the molecular weight of the solute and C_0 the initial concentration of the solute in the raw water.

Speigler and Kedem [27] use of the above equation expresses the retention rate of the solute as a function of permeate flux:

$$\mathrm{TR} = \sigma\frac{1-F}{1-\sigma F} \quad (6)$$

With:

$$F = \exp\left(-\frac{1-\sigma}{P_s}J_v\right) \quad (7)$$

It is worth noting that Eq. (7) is called Speigler–Kedem equation. According to relations (6) and (7), the retention rate of TR increases with increasing water flux and reached a limit value equal to σ when the flux tends to infinity (maximum retention that could be obtained at high pressure), as reported recently [29]. P_s being the diffusive flux of solute when the solvent flux tends to 0.

The parameter σ was calculated from the relationship Pusch [32]:

$$\frac{1}{\mathrm{TR}} = \frac{1}{\sigma} + \left(\frac{L_D}{L_p} - \sigma^2\right)\frac{L_p \cdot \pi_1}{\sigma \cdot J_v} = A_1 + A_2 \cdot \frac{1}{J_v} \quad (8)$$

where L_D represents the osmotic permeability coefficient.

The graphic representation of 1/TR vs. $1/J_v$ allows us to determine the value of σ. Speigler–Kedem approach was usually applied when there was no electrostatic interaction between membrane and solute. This is the case when the membrane is uncharged such as RO membrane or when the solute is neutral (organic compounds). Many authors [29,33,34] used this model with a nanofiltration membrane that is charged, the parameters $\bar{\sigma}$ and P_s depend on the membrane effective charged and the concentration of feed solute solution.

3. Materials and methods

3.1. Reverse osmosis membrane and chemicals

The membrane under study was a spiral wound aromatic polyamide thin film composite denoted SG from GE Osmonics Company. An overview of the membrane properties, as indicated by manufacturer, is given in Table 1.

Before use, the membrane was soaked in water for 24 h in order to eliminate conservation products. The pure water permeability was determined.

Four common salts (NaCl, $CaCl_2$, Na_2SO_4, and $NaNO_3$) were chosen to provide charged solute species in order to determine the membrane desalting degree.

Phenol was synthesis grade, purchased from FLUKA, and used without further purification. Table 2 summarizes some relevant physicochemical properties of organic compound.

Table 1
Main characteristics of the membrane used in the experimental test module

	Membrane
Manufacturer	GE Osmonics
Product denomination	SG
Type	Thin film composite
Composition	Polyamide
Effective membrane surface area (m^2)	0.6
Module	Length 14 inch Diameter 2.5 inch
Maximum pressure (bar)	40
Maximum temperature (°C)	50
NaCl rejection	98.2
pH tolerance	4–11

Table 2
Physico-chemical properties of phenol [35,36]

Molecular weight ($g.mol^{-1}$)	94.11
Water solubility ($g.L^{-1}$)	93 at 25°C
pK_a	9.95
Molecular width (Å)	2.66
Formula	C_6H_5OH

Synthetic solutions are prepared by adding required amounts of phenol to distilled water. The feed solutions are prepared with different concentration of phenol ranged from 10 to 2000 $mg.L^{-1}$. NaOH and HCl were used to adjust the pH of feed solutions.

3.2. Procedure

The experiments were performed on a pilot plant, which was carried out in our laboratory and equipped with RO modules in order to investigated phenol removal.

The flow diagram of the pilot plant unit is shown in Fig. 1.The experimental RO system consisted of a polyamide membrane kept inside a stainless steel cylindrical housing capable of withstanding high pressures. A feed tank of 60 L capacity is provided for storage and supply of the feed to the system as well as for the collection of the recycled permeate and retentate. A high-pressure pump capable of developing a pressure up to 30 bar was installed for transporting the feed liquid through the membrane system. Manual needle valves were provided to pressurize the feed liquid to a desired pressure indicated by pressure

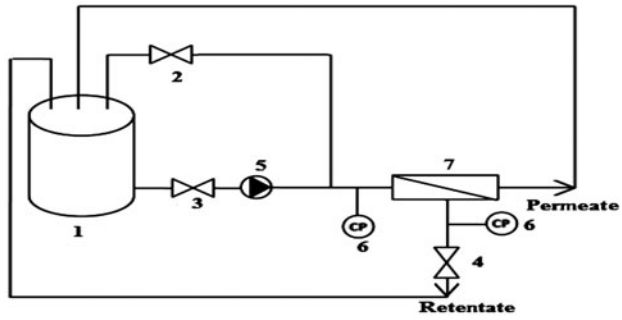

Fig. 1. Schematic of the experimental RO system. 1: Feed tank; 2: recirculation valve; 3: valve; 4: reject valve; 5: pump; 6: pressure gauges; 7: RO membrane module.

gauges installed in both the feed and retentate lines. Operation was in a recycle mode, that is, the retentate as well as permeate was recycled to the feed tank. In each experiment, a 15 L of phenol solution was permeated at a fixed pressure (P = 3, 4, 5, 6, 7, 8, 9, 10, and 11 bar). Samples permeate was taken at regular intervals during the run and the unit was operated for sufficient time to ensure steady state conditions. The membrane system was first run with ultrapure water to determine the initial membrane pure water permeability. Following each experiment, the membrane was cleaned with ultrapure water at 5 bar. After each set of experiments for a given feed concentration, the setup was rinsed with distilled water for 30 min at 5 bar to clean the system. This procedure was followed by measurement of pure water permeability with distilled water to ensure that the initial membrane is restored. When necessary, a sodium bisulfite was used as cleaning agent. The permeate flux was determined by measuring the permeate volume corresponding to 5 s. Experiments were done at room temperature.

Thus, the membrane retention R is approximately equal to observed retention and is defined as:

$$TR = 1 - \frac{C_p}{C_f} \tag{9}$$

where C_p and C_f are permeate and feed concentrations, respectively.

Permeate flux J_v ($L.h^{-1}.m^{-2}$) was calculated as follows:

$$J_v = \frac{v}{t \cdot S} \tag{10}$$

where *V(L)* is the volume of permeate collected within time *t(h)* and *S* is the membrane area (m^2).

The recovery rate Y is given as:

$$Y\% = \left(\frac{Q_p}{Q_0}\right) \times 100 \quad (11)$$

where Q_0 and Q_p are the initial and permeate flow rates, respectively.

The recovery rate was fixed by adjusting the two valves V2 and V3 and by measuring each time the flow rates of permeate Q_p and retentate Q_r (the flow measurement is achieved by measuring the volumes V_p and V_p per unit of time:($Q_P = \frac{V}{\Delta t}$ $(L \cdot h^{-1})$). The conversion rate is the ratio of the permeate flow rate to the flow rate of the feed water entering the feed water tank.

3.3. Analytical methods

Concentration of inorganic salts NaCl, Na_2SO_4, $NaNO_3$, and $CaCl_2$ was measured by conductivity (Metrohm 712). The phenol concentrations in feed and permeate solutions were determined spectrophotometrically at 270 nm. A spectrophotometer model TOMOS V-1100 was used for colorimetric analysis. The calibration plot of absorbance versus concentration for phenol showed a linear variation up to 60 mg.L^{-1} concentration. Therefore, the samples with higher concentration of phenol (>60 mg.L^{-1}) were diluted with distilled water, whenever necessary. The pH of the aqueous solution of phenol varied from 5.5 to 6 for the phenol concentration varying from 10 to 2,000 mg.L^{-1}.

4. Results and discussion

4.1. Membrane characterization

The manufacturers of the membranes generally give very little information on their products for understandable reasons to protect their secret, and it is difficult to compare the data because they have not been established in same operating conditions. The characteristics of membranes indicated by the manufacturers were insufficient to justify the choice of a membrane for a particular application. Hydraulic tests were required for better characterization of such membranes. Desalting degree constitutes another suitable parameter often used for the characterization of the retention properties of RO membranes.

4.1.1. Water permeability

Before the actual experimentation, the pure water permeability of the membrane using distilled water is measured at 25°C to characterize the membrane. The flux solvent evolution of pure water with the transmembrane pressure across RO membrane was reported in Fig. 2. The linear evolution of flux with the transmembrane pressure shows that Darcy's law is verified and the mean value of L_p was 2.8 L.h^{-1}.m^{-2}.bar^{-1}. The L_p value was used as a reference to evaluate cleaning procedures, concentration polarization, and membrane fouling.

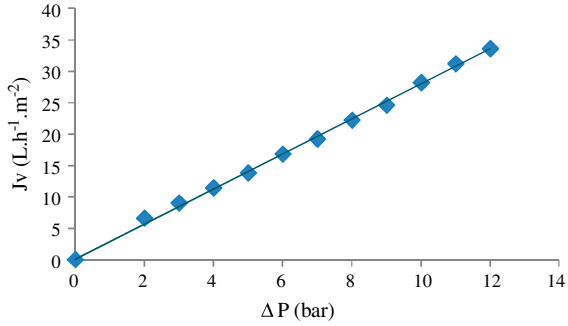

Fig. 2. Permeate flux as a function of applied pressure at $T = 25$°C.

4.1.2. Salt retention measurements

The interest in knowing of the salt retention measurements is to understand the mechanisms governing ion retention by membranes. The salt retention measurements showed that the behavior of most of the membranes could be classified into two main categories:

- Membranes for which Donnan exclusion seems to play an important role.
- Membrane for which the retention was determined by difference in diffusion coefficients between the salts.

Three salts were chosen to span a variety electrolyte types including symmetric 1–1 electrolyte (NaCl) as well as asymmetric 2–1 and 1–2 electrolytes ($CaCl_2$ and Na_2SO_4).

The retention of these three salts at a concentration of 10^{-3} mol.L^{-1} by the RO membrane as a function of permeate flux is given in Fig. 3. It clear that rejection is nearly constant with permeate flux for Na_2SO_4 while for NaCl and $CaCl_2$ the rejection increases with increasing flux and tends to plateau. From this figure, it can be seen that the membrane shows the following salt rejection sequence: $TR_{Na_2SO_4} > TR_{CaCl_2} > TR_{NaCl}$ indicated that the retention is mainly caused by difference in diffusion coefficients between three salts [35]. As shown in Table 3, the diffusion coefficient decreases from NaCl, $CaCl_2$ to Na_2SO_4. This order of diffusion

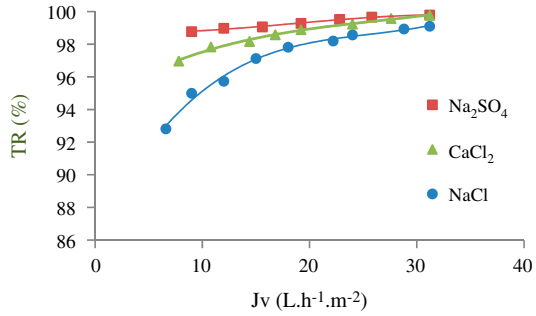

Fig. 3. Variation of rejection rate of salts ($C = 10^{-3}$ mol.L^{-1}) as a function of water flux.

Table 3
Diffusion coefficients of different electrolytes in water [37]

Electrolyte	D (10^{-9} m^2.s^{-1})
NaCl	1.61
$CaCl_2$	1.45
Na_2SO_4	1.23

coefficients is inversely reflected in the retention sequence. The salt with the lowest diffusion coefficient shows the highest retention, whereas that with the highest diffusion coefficient shows the lowest retention.

According to the sequence of retention mentioned above, we can conclude that:

$$TR_{Ca^{2+}} > TR_{Na^{+}} \quad \text{and} \quad TR_{SO_4^{2-}} > TR_{Cl^{-}}$$

Thus, we find that the sulfate anion SO_4^{2-} (bivalent) is better retained than chloride anion Cl^- (monovalent) and the calcium cation Ca^{2+} (bivalent) is better retained than the sodium cation Na^+ (monovalent).

From Table 4, we find that the retention of salts may be related to the difference in hydration energies of ions which indicate the existence of the steric effect on retention. Indeed, the ions, which have higher hydration energy, are more retained. The polyvalent ions, which have a higher energy of hydration, are better retained than less hydrated monovalent ions as is the case with sulfate anions relative to chloride anions and cations calcium relative to sodium cations.

4.1.3. Evaluation of diffusion and convection flux of solute

For a better understanding of transport phenomena of salt in membrane, it is possible to evaluate the

Table 4
Hydratations energies of different electrolytes [38]

Ions	Hydratation energy (kJ.mol^{-1})
Na^+	454
Ca^{2+}	1,615
Cl^-	325
SO_4^{2-}	1,047
NO_3^-	310

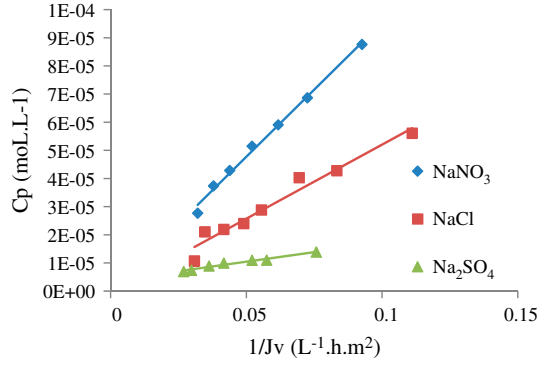

Fig. 4. Variation of the permeate concentration in function of $\frac{1}{Jv}$ for different salts, $C = 10^{-3}$ mol.L^{-1}, pH = 6.5.

dual phenomena of transfer, that is, transfer by convection and diffusion. To determine experimentally the values of the diffusion flux J_{diff} and concentration C_{conv} of solute selectively entrained by convection, we present the concentration of the permeate Cp according to the reverse flux $1/J_v$ for the three salts NaCl, $NaNO_3$, and Na_2SO_4 at a concentration of 10^{-3} mol.L^{-1} (Fig. 4).

The curves obtained are straight linear and satisfy well the relation (6). For high values of flux, that is, when 1/Jv tends to zero, we obtain the amount of mass transfer of solute corresponding to the convective part C_{conv} and the slope of the diffusive flux in J_{diff}. This allows evaluating simultaneously by mass transfer of solute due to chemical phenomena and convective part derived from a purely physical mechanism. To modulate the selectivity of the membrane toward the solutes, it is possible to favor one or the other mechanism by varying the operating parameters. Some physical parameters such as pressure, recovery rate, etc., can greatly influence the mass transfer by convection, whereas some parameters such as concentration can influence the mass transfer by diffusion.

The values of the parameters of J_{diff} and C_{conv} are grouped in Table 5.

Table 5
Values of C_{conv} and J_{diff} obtained for single salt at concentration 10^{-3} mol. L^{-1}

Salts (10^{-3}mol.L^{-1})	J_{diff} (L.h^{-1}.m^{-2})	C_{conv} (mol.L^{-1})
$NaNO_3$	10^{-3}	10^{-7}
NaCl	5×10^{-4}	7×10^{-7}
Na_2SO_4	10^{-4}	4×10^{-6}

Table 6
Reflexion coefficient (σ) and permeability (P_s) of three sodium salts

Salts (10^{-3} mol.L^{-1})	σ	P_s
$NaNO_3$	0.992	0.964
NaCl	0.995	0.436
Na_2SO_4	0.996	0.149

Table 5 shows that the values of J_{diff} are in reverse to the hydration energy order (Table 4). The order of J_{diff} values of different electrolytes is as follows: $SO_4^{2-} < Cl^- < NO_3^-$.

In the RO membrane, the solute transport is carried out by diffusion, since the values of C_{conv} are very low.

4.1.4. Molecular weight cutoff (MWCO) membrane determination from C_{conv} data

From the C_{conv} values, it is possible, using the following equation $C_{conv} = C_0\left[1 - (M/\mathrm{MWCO})^{\frac{1}{3}}\right]^2$, to calculate the molecular cutoff of the membrane studied, using a divalent electrolyte such as Na_2SO_4 at a concentration of 10^{-3}mol.L^{-1}. However, the most appropriate values are those obtained at low concentrations where the retention of Na_2SO_4 is higher than 90% (Fig. 3). The value of the MWCO obtained for the SG membrane is 173 Dalton.

4.1.5. Determination of transport parameters

The transport parameters Ps and σ were determinate using the Speigler–Kedem model. The plot of 1/TR based on $1/J_v$ allows us to determine the values of σ. In the case of SG membrane, three salts have been used NaCl, $NaNO_3$, Na_2SO_4 at a concentration of 10^{-3}mol.L^{-1}. Fig. 5 represents the variation of the inverse of retention rates as in function of to the reverse flux for different salts. The curves are also straight line and verifying well the relation (8). The value of σ corresponds to the inverse of the origin of the curve $1/TR = f(1/J_v)$.

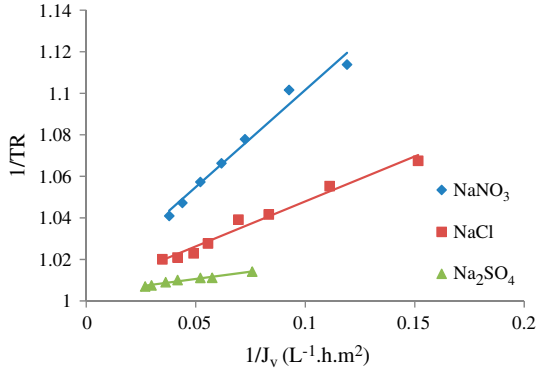

Fig. 5. Variation of $\frac{1}{TR}$ in function of $\frac{1}{lv}$ for different salts, $C = 10^{-3}$ mol.L^{-1}, pH = 6.5. The results obtained were summarized in Table 6.

These results revealed that Ps values are highly dependent on the type of anion of the electrolyte solution. Strongly solvated anions (SO_4^{2-}) lead to lower values of P_s in comparison with less solvated anions (NO_3^-). The reflection coefficient is higher for the sulfate ions. It also appears that the reflection coefficient increases with increasing energy of hydration.

4.2. Phenol retention

4.2.1. Effect of transmembrane pressure on phenol retention and permeate flux

As RO is usually a pressure-driven process, operating pressure is very important factor affecting rejection performance. To investigate the influence of applied pressure on the rejection of phenol, the pressures were varied from 3 to 9 bar at a pH of 6 and a feed concentration of 50 mg.L^{-1}. The effect of operating pressure on the rejection of phenol is presented in Fig. 6.

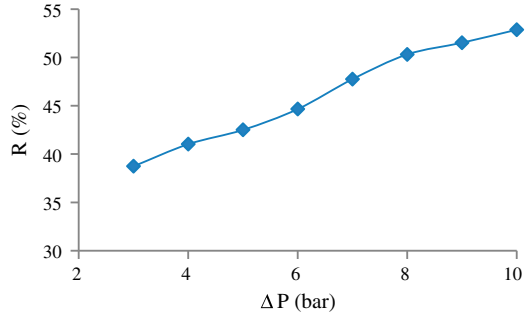

Fig. 6. Effect of pressure on the retention of phenol, $C = 50$ mg.L^{-1}, $Y = 20\%$, pH = 6.5.

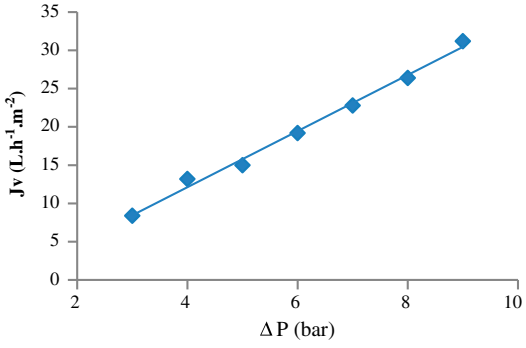

Fig. 7. Effect of pressure on permeate flux of phenol, $C = 50\,mg.L^{-1}$, $Y = 20\%$, pH = 6.5.

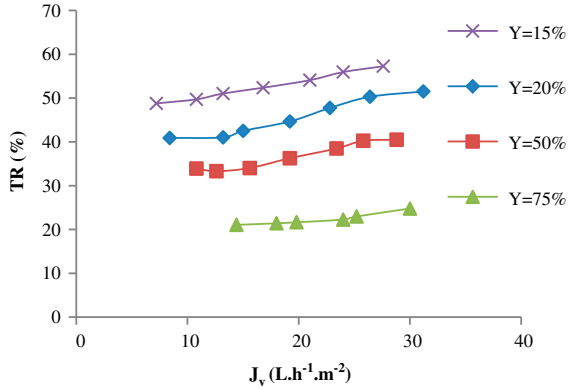

Fig. 8. Effect of recovery rate on the retention of phenol, $C = 50\,mg.\,L^{-1}$, pH = 6.5.

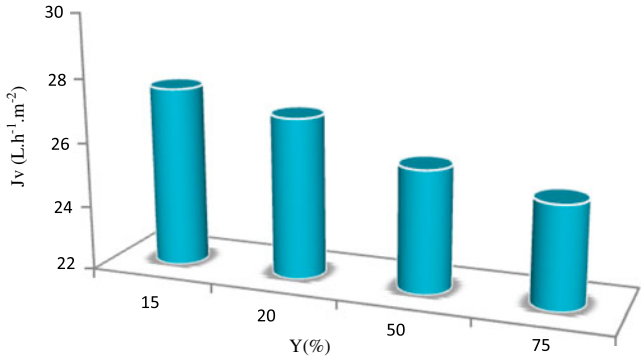

Fig. 9. Effect of recovery rate on permeate flux of phenol, $C = 50\,mg.\,L^{-1}$, pH = 6.5, P = 9 bar.

As can be seen from Fig. 6, the phenol rejection increased with increasing the operating pressure. The investigation shows that the observed rejection of phenol increases from 38 to 53%. This phenomenon could be attributable to the increased solvent flux at a higher pressure [39]. Actually, permeate flux increase with pressure corresponds to an enhanced transfer of water through the membranes compared to the solutes one, which depends largely on concentration difference across the membrane, leading to the dilution of the latter in permeate and to their concentration in retentate. Hence, the observed rejection increases with increasing pressure.

Fig. 7 shows that the permeate flux varies linearly with the transmembrane pressure. A shift of the right of J_v as function of the pressure from the origin to the high pressures was observed indicating the presence of an osmotic pressure. Indeed, the osmotic pressure $\Delta\pi$ is the difference of osmotic pressure of both sides of the membrane, that is to say between the retentate and the permeate. Effective pressure is lower than the applied pressure, and flux is reduced accordingly.

4.2.2. *Effect of recovery rate on phenol retention and permeate flux*

In real applications, NF and RO operations will be operated at high recovery rates since at higher the recovery more permeate is obtained. The influence of recovery rate on RO membranes was investigated and results are presented in Fig. 8.

Fig. 8 shows that the phenol rejection decreases with increase in recovery rate for the SG membrane. Many authors have reported that an increase in recovery rate leads to a decrease in rejection [40–42]. This is attributed to the effect of the reduction in the speed of tangential circulation and of the apparition of the concentration polarization, which occurs due to the accumulation of retained solutes at the membrane–solution interface, at higher recovery rate.

On the other hand, from Fig. 9, the permeate flux decreases with increasing conversion rate and concentration of solutes near the membrane in the compartment of the solution becomes important, this causes an increase in transfer of solutes to the other side of the membrane, and the concentration of solute in the permeate became greater. Hence, the retention rate would be lower.

4.2.3. *Effect of feed concentration on phenol retention and permeate flux*

To determine the extent to which the retention of phenol is influenced by feed concentration, phenol was prepared at various concentrations, such as 10, 50, 500, 1,000, and 2,000 mg. L^{-1}.

Fig. 10 shows the effect of the phenol feed concentration on the observed retention. The findings show that the retention rate of phenol increases as the feed

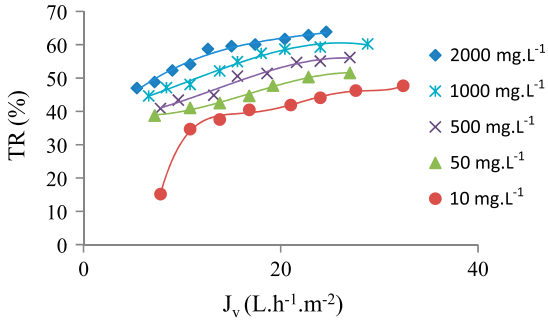

Fig. 10. Effect of feed concentration on the retention of phenol, $Y = 20\%$, pH = 6.5.

Table 7
Reflexion coefficient (σ) and permeability (P_s) for phenol at various concentrations

Phenol (mg.L^{-1})	σ	P_s (L.h^{-1}.m^{-2})
10	0.578	11.08
50	0.627	9.23
500	0.662	7.64
1,000	0.676	5.82
2,000	0.705	4.67

concentration increase. We can explain this by the fact that increasing the feed concentration of phenol leads to an increase in the amount of phenol in the permeate, but as the increase in permeate concentration is lower than the increase in feed concentration, the retention rate increases in accordance with the following equation $R = 1 - \frac{C_p}{C_a}$ [43].

The membrane parameters σ and Ps of phenol are summarized in Table 7.

According to Table 7, we find that the transport parameters σ and P_s depend on the concentration of phenol: the reflection coefficient increases slightly with the concentration due to the increase in the phenol rejection, while the solute permeability Ps decreases with the concentration of phenol due to the little amount of phenol passing through the membrane.

Fig. 11 represents the variation of feed concentration of phenol vs. the permeate flux. It appears that the permeate flux of phenol decreases as the phenol concentration increases for any particular pressure. This variation of flux with concentration is attributed to the increase in osmotic pressure with increase in feed concentration which causes a reduction in the driving force ($\Delta P - \Delta\pi$) for the permeation of solvent across the membrane and a subsequent decrease in the permeate flux [44].

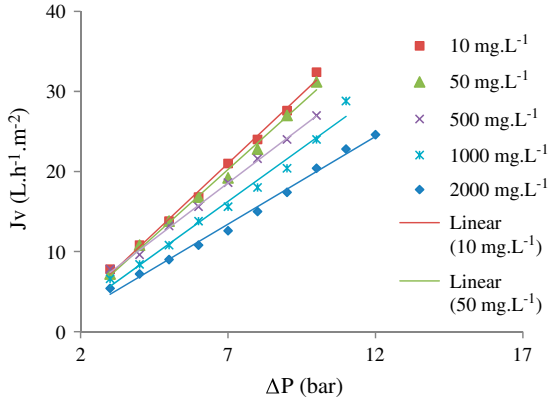

Fig. 11. Effect of feed concentration on the permeate flux, $Y = 20\%$, pH = 6.5.

4.2.4. Effect of pH on phenol retention and permeate flux

The pH is an important operational variable in the treatment of phenol; the pH is also one of the factors that influence the retention rate. In general, when a compound is partially ionized or charged carrier functions, consider the electrostatic interactions that can occur between the membrane and the solutes.

Phenol, an organic acid, was dissociated with regard to the pH in the solution as follows:

$$C_6H_5OH + H_2O \rightleftharpoons C_6H_5O^- + H_3O^+ pK_a = 9.95$$

Dissociation of phenol C_6H_5OH to phenolate $C_6H_5O^-$ at $pK_a = 9.95$. Based on above equation, within the pH below 9.95, the phenol predominantly existed in aqueous solution as neutral form (C_6H_5OH). In addition, the anionic form of phenol ($C_6H_5O^-$) increased with an increase in pH value above 9.95. Generally, rejection of weak acids and bases is highly pH dependent; their retention in RO process will be high in the ionized form. Thus, the organic acid rejection increases significantly at pH levels above the acidity constant (pKa), but the rejection decreases at pH levels below pKa (where the acid are in the neutral form).

The effect of pH on the retention of phenol was studied at fixed concentration 50 mg.L^{-1} and at transmembrane pressure 7 bar. The pH was adjusted using chloride acid (HCl) or sodium hydroxide (NaOH). The results plotted with the theoretical diagram of phenol speciation are given in Fig. 12.

Phenol retention (shown in Fig. 12) was impacted significantly by pH. Retention was approximately 50% between pH 5 and 9. At pH 10 and 11, retention

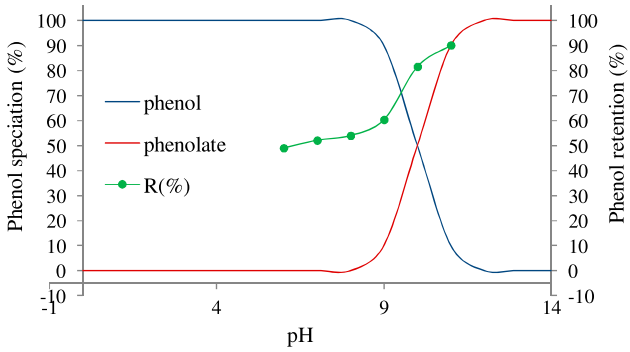

Fig. 12. Effect of pH on the retention of phenol, $C = 50\,mg.L^{-1}$, $Y = 20\%$, $P = 7\,bar$.

increased significantly. Similar pH effects on phenol retention have been previously reported [45]. In addition the retention pattern correlated closely with speciation of phenol. At acidic and neutral pH, where retention is lowest, only phenol was present. This neutral species was easily transported through the membrane due both to lack of steric hindrance and lack of charge repulsion. At pH ⩾ 9, retention increased sharply (up to 90%). The increase in retention closely corresponded with the speciation change from phenol to phenolate (see Fig. 12), which is anionic as opposed to phenol. In consequence, the increase in concentration of dissociated phenolic species, negatively charge, and the enhancement of the surface membrane negative charge with pH strengthen the electrostatic repulsion between the membrane and charged solutes.

From Fig. 13, at a feed concentration of $50\,mg.L^{-1}$, a recovery rate of 20% and a transmembrane pressure of 7 bar, the permeate flux was independent of pH. This result was obtained by other authors [43,46].

4.2.5. Effect of ionic strength on phenol retention and permeate flux

Really, industry effluents contain a high concentration of salts; in fact, the ionic strength is a parameter that influences the retention of phenol. To investigate the effect of salts on the rejection of phenol for the employed RO membranes, rejection experiments were performed by the addition of various concentrations of NaCl between 0.001 and 0.1 M in phenol solution (phenol concentration = $50\,mg.L^{-1}$, pH = 11. Fig. 14 shows that the increase in salt concentration leads to a decrease in the retention of phenol. The retention of phenol decreases from 94 to 81% when the concentration of NaCl increases from 0 to $10^{-1}\,mol.L^{-1}$. This decrease can be attributed to the increase in ionic strength screen the charges provided by the membrane which reduces the electrostatic interactions and therefore reduce the retention of phenol. Indeed, the added sodium ions partially neutralize the negative charge of the membrane which results in a weakening of the repulsion between phenol (present the phenolate anion at pH = 11) and the membrane.

Thus, the increased salinity induces a decrease in electrostatic interactions by shielding of charged sites, leading to a weakening of retention. Conversely, an improvement in retention can be observed at very low ionic strength.

The transport parameters б and P_s are listed in Table 8. It clears that values of P_s and σ are dependent on the NaCl concentration; P_s increases while б slightly decreases with salt concentration.

Fig. 15 shows the variation of the permeate flux as a function of the applied pressure at various concentrations of NaCl, phenol concentration $50\,mg.L^{-1}$, $Y = 20\%$, and pH = 11. It shows that the permeate flux

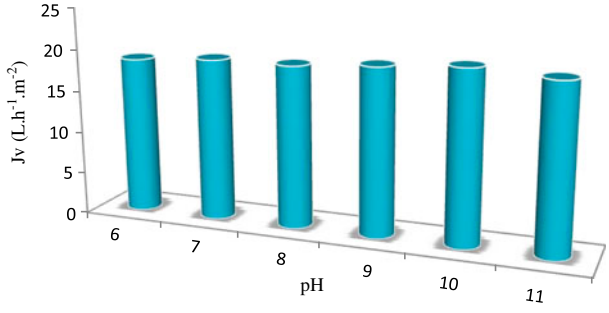

Fig. 13. Effect of pH on the permeate flux, $C = 50\,mg.L^{-1}$, $Y = 20\%$, $P = 7\,bar$.

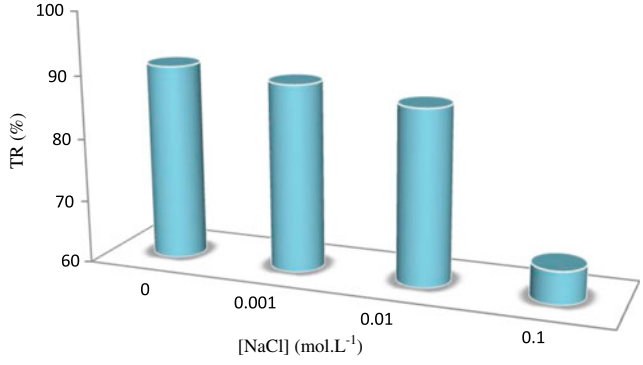

Fig. 14. Effect of ionic strength on the retention of phenol, $C = 50\,mg.L^{-1}$, $Y = 20\%$, pH = 11, $P = 7\,bar$.

Table 8
Reflexion coefficient σ and permeability (P_s) for phenol ($C = 50\,mg.L^{-1}$) at different NaCl concentrations

NaCl (mol.L^{-1})	σ	P_s (L.h^{-1}.m^{-2})
0	0.965	1.40
10^{-3}	0.956	1.77
10^{-2}	0.951	2.12
10^{-1}	0.949	3.25

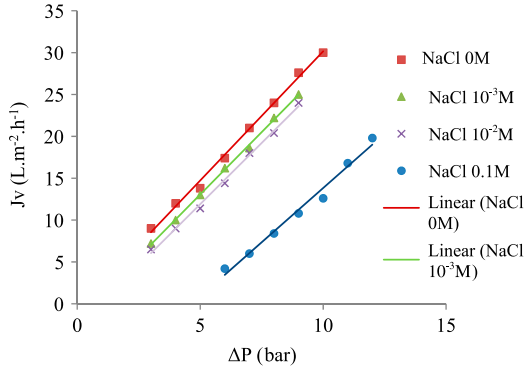

Fig. 15. Effect of ionic strength on permeate flux, $C = 50\,mg.L^{-1}$, $Y = 20\%$, pH = 11, P = 7 bar.

at a given pressure depends on NaCl concentration, which is due to the osmotic effect.

5. Conclusion

Characterization of RO membrane was performed and subsequently the feasibility of phenol removal was investigated. The determined pure water permeability of the SG membrane was 2, 8 L.h^{-1}.m^{-2}.bar^{-1}. The sodium salts retention sequence was $TR_{Na_2SO_4} > TR_{CaCl_2} > TR_{NaCl}$ which indicate that the retention was mainly caused by differences in diffusion coefficients between the different salts. The value of the MWCO obtained for the SG membrane was 173 D. The results deducted from the phenomenological model confirm that for the SG membrane the transfer is purely diffusionnel. Phenomenological parameters σ and P_s were calculated. They depend highly on the type of anion of the electrolyte.

The removal efficiency for phenol was influenced by the operating conditions such as transmembrane pressure, recovery rate, feed concentration, pH, and ionic strength. It is observed that the rejection of phenol increases with increase in transmembrane pressure and decreases with increase in recovery rate. The observed rejection depend on the feed concentration, in fact, an increase in feed concentration leads to an increase on phenol retention. Phenol retention increased with increase in pH due to electrostatic repulsion between membrane and phenolate. Additionally, when ionic strength increases, phenol rejection decreases due to the shielding phenomenon. The results of the application of Speigler–Kedem model show that there was a good agreement between theoretical and experimental curves.

Abbreviations

C_0	—	solute concentration in feed (mol.L^{-1})
C_{conv}	—	solute concentration due to convection (mol.L^{-1})
C_f	—	solute concentration in the feed (mol.L^{-1})
C_m	—	solute concentration at the surface membrane
C_p	—	solute concentration in the permeate (mol. L^{-1})
D	—	diffusion coefficient (m^2.s^{-1})
J_{diff}	—	solute flux due to diffusion (L.h^{-1}.m^{-2})
J_s	—	solute flux (L.h^{-1}.m^{-2})
J_v	—	permeate flux (L.h^{-1}.m^{-2})
L_D	—	osmotic permeability coefficient
L_p	—	pure water permeability (L.h^{-1}.m^{-2}.bar^{-1})
M	—	molecular weight of a solute (g.mol^{-1})
MWCO	—	molecular weight cut off (Dalton)
Pc	—	critical pressure (bar)
P_s	—	solute permeability versus membrane (L.h^{-1}.m^{-2})
Q_0	—	initial flow rate
Q_p	—	permeate flow rate
R	—	retention (%)
TR	—	retention rate (%)
Y	—	recovery rate (%)
ΔP	—	transmembrane pressure (bar)
$\Delta\pi$	—	osmotic pressure difference across membrane (bar)
σ	—	reflexion coefficient

References

[1] P. Venkateswaran, K. Palanivelu, Recovery of phenol from aqueous solution by supported liquid membrane using vegetable oils as liquid membrane, J. Hazard. Mater. 131 (2006) 146–152.
[2] O. Abdelwahab, N.K. Amin, E.-S.Z. El-Ashtoukhy, Electrochemical removal of phenol from oil refinery wastewater, J. Hazard. Mater. 163 (2009) 711–716.
[3] G. Bayramoglu, M.Y. Arica, Enzymatic removal of phenol and p-chlorophenol in enzyme reactor: Horseradish peroxidase immobilized on magnetic beads, J. Hazard. Mater. 156 (2008) 148–155.
[4] O. Tepe, A.Y. Dursun, Combined effects of external mass transfer and biodegradation rates on removal of phenol by immobilized Ralstonia eutropha in a packed bed reactor, J. Hazard. Mater. 151 (2008) 9–16.
[5] Agency for Toxic Substances and Disease Registry (ATSDR), Toxicological Profile for Phenol, US Department of Health and Human Services, Public Health Service, Atlanta, GA, 1998.

[6] World Health Organization, Health Criteria and Supporting Information, WHO Guidelines for Drinking Water Quality (vol. II), Geneva, Switzerland, 1984.
[7] N.N. Dutta, S. Brothakur, R. Baruaha, A novel process for recovery of phenol from alkaline wastewater: Laboratory study and predesign cost estimate, Water. Environ. Res. 70 (1998) 4–9.
[8] C.P. Das, N.L. Patnaik, Removal of phenol by industrial solid waste, Pract. Period. Haz. Toxic. Radioac. Waste Manag. 9(2) (2005) 135–140.
[9] M. Carmona, A. de Lucas, J.L. Valverde, B. Velasco, J.F. Rodríguez, Combined adsorption and ion exchange equilibrium of phenol on Amberlite IRA-420, Chem. Eng. J. 117(2) (2006) 155–160.
[10] Y.M. Awad, N.S. Abuzaid, The influence of residence time on the anodic oxidation of phenol, Sep. Purific. Technol. 18 (2000) 227–236.
[11] B. Seredynska-Sobecka, M. Tomaszewska, A.W. Morawski, Removal of micropollutants from water by ozonotation/biofiltration process, Desalination 182(1–3) (2005) 151–157.
[12] G. Dursun, C. Handan, Y.D. Arzu, Adsorption of phenol from aqueous solution by using carbonised beet pulp, J. Hazard. Mater. B 125 (2005) 175–182.
[13] C.F. Schutte, The rejection of specific organic compounds by reverse osmosis membranes, Desalination 158(1–3) (2003) 285–294.
[14] J.M. Arsuaga, M.J. López-Muñoz, A. Soto, G. del Rosario, Retention of phenols and carboxylic acids by nanofiltration/reverse osmosis membranes: Sieving and membrane-solute interaction effects, Desalination 200(1–3) (2006) 731–733.
[15] A. Ben-David, S. Bason, J. Jopp, Y. Oren, V. Freger, Partitioning of organic solutes between water and polyamide layer of RO and NF membranes: Correlation to rejection, J. Membr. Sci. 281(1–2) (2006) 480–490.
[16] E.S.K. Chian, W.N. Bruce, H.H.P. Fang, Removal of pesticides by reverse osmosis, Environ. Sci. Technol. 9 (1975) 52–59.
[17] K. Kimura, G. Amy, J.E. Drewes, T. Heberer, T.U. Kim, Y. Watanabe, Rejection of organic micro pollutants (disinfection by-products, endocrine disrupting compounds and pharmaceutically active compounds) by NF/RO membranes, J. Membr. Sci. 227 (2003) 113–121.
[18] P. Xu, J.E. Drewes, C. Bellona, G. Amy, T.U. Kim et al., Rejection of emerging organic micro pollutants in nanofiltration-reverse osmosis membrane applications, Water Environ. Res. 77 (2005) 40–48.
[19] C. Bellona, J.E. Drewes, P. Xu, G. Amy, Factors affecting the rejection of organic solutes during NF/RO treatment-a literature review, Water Res. 38 (2004) 2795–2809.
[20] Y. Yoon, R.M. Lueptow, Removal of organic contaminants by RO and NF members, J. Membr. Sci. 261 (2006) 76–86.
[21] A. Bodalo-Santoyo, J.L. Gomez-Carasco, E. Gomez-Gomez, M.F. Maximo-Martin, A.M. Hidalgo-Montesinos, Spiral-wound membrane reverse osmosis and the treatment of industrial effluents, Desalination 160 (2004) 151–158.
[22] V.V. Goncharuk, D.D. Kucheruk, V.M. Kochkodan, V.P. Badekha, Removal of organic substances from aqueous solutions by reagent enhanced reverse osmosis, Desalination 143 (2002) 45–51.
[23] B. Van der Bruggen, J. Schaep, D. Wilms, C. Vandecasteele, Influence of molecular size, polarity and charge on the retention of organic molecules by nanofiltration, J. Membr. Sci. 156 (1999) 29–41.
[24] B. Van der Bruggen, L. Braeken, C. Vandecasteele, Evaluation of parameters describing flux decline in anofiltration of aqueous solutions containing organic compounds, Desalination 147 (2002) 281–288.
[25] C. Sagne, C. Fargues, B. Broyart, M.L. Lameloise, M. Decloux, Modeling permeation of volatile organic molecules through reverse osmosis spiral-wound membranes, J. Membr. Sci. 330 (2009) 40–50.
[26] N. Yinyip, A. Tiraferri, W. Phillip, J. Schiffman, M. Elimelech, High performance Thin-Film Composite forward Osmosis Membrane, Environ. Sci. Technol 44 (2010) 3812–3818.
[27] K.S. Spiegler, O. Kedem, Thermodynamics of hyperfiltration (reverse osmosis): Criteria for efficient membrane, Desalination 1 (1966) 311–326.
[28] M. Pontié, H. Dach, J. Leparc, M. Hafsi, A. Lhassani, Novel approach combining physico-chemical characterizations and mass transfer modelling of nanofiltration and low pressure reverse osmosis membranes for brackish water desalination intensification, Desalination 221 (2008) 174–191.
[29] C.K. Diawara, S.M. Lo, M. Rumeau, M. Pontie, O. Sarr, A phenomenological mass transfer approach in nanofiltration of halide ions for a selective defluorination of brackish drinking water, J. Membr. Sci. 219 (2003) 103–112.
[30] M. Pontié, C.K. Diawara, M. Rumeau, Streaming effect of single electrolyte mass transfer in nanofiltration: Potential application for the selective defluorination of brackish drinking waters, Desalination 151 (2003) 267–274.
[31] A. Lhassani, M. Rumeau, D. Benjelloun, Essai d'interprétation des mécanismes de transfert des sels en nanofiltration [Interpretation attempt of transfer mechanism of salt in nanofiltration], Tribune de l'eau 53 (2000) 100–107.
[32] J.J. Gilron, N. Gara, O. Kedem, Experimental analysis of negative salt rejection in nanofiltration membranes, J. Membr. Sci. 185 (2001) 223–236.
[33] A. Hafiane, D. Lemordant, M. Dhahbi, Removal of hexavalent chromium by nanofiltration, Desalination 130 (2000) 305–312.
[34] W. Pusch, Determination of transport parameters of synthetic membranes by hyperfiltration experiments, Part I: Derivation of transport relationship from linear relations of thermodynamics of irreversible process, Ber. Bunsenges. Phys. Chem. 81(3) (1977) 269–276.
[35] Kirk-Othmer, Concise Encyclopedia of Chemical Technology, fourth ed., Wiley, New York, 1999, pp. 1514.
[36] W. Jordan, H. van Barneveld, O. Gerlich, M. Kleine-Boymann, J. Ullrich, Phenol, in: Ullmann's Encyclopedia of Industrial Chemistry, Wiley-VCH Verlag, 2002.
[37] J.M.M. Peeters, J.P. Boom, M.H.V. Mulder, H. Strathmann, Retention measurements of nanofiltration membranes with electrolyte solutions, J. Memb. Sci. 145 (1998) 199–209.
[38] J. Schaep, C. Vandecasteele, A. Wahab Mohammad, W. Richard Bowen, Modeling the retention of ionic components for different nanofiltration membranes, Sep. Purif. Technol. 22–23 (2001) 169–179.
[39] J.H. Choi, K. Fukushi, K. Yamamoto, A study on the removal of organics acids from wastewater using nanofiltration membranes, Sep. purif. technol. 59 (2008) 17–25.
[40] A.H. Bannoud, Elimination de la dureté et des sulfates contenus dans les eaux par nanofiltration [Elimination of hardness and sulfate content in water by nanofiltration], Desalination 137 (2001) 133–139.
[41] A. Lhassani, M. Rumeau, D. Benjelloun, M. Pontié, Selective demineralization of water by nanofiltration, Appl. defluorination brackish water, Water Res. 35 (2001) 3260–3264.
[42] A. Abouzaid, A. Mouzdahir, M. Rumeau, Etude de la rétention des sels monovalents et bivalents par nanofiltration [Study of the retention of monovalent and bivalent salts by nanofiltration], Comptes Rendus de Chimie 6 (2003) 431–436.
[43] J.L. Gomez, G. Leon, A.M. Hidalgo, M. Gomez, M.D. Murica, G. Grinan, Application of reverse osmosis to remove aniline from wastewater, Desalination 245 (2009) 687–693.
[44] Z.V.P. Murthy, S.K. Gupta, Estimation of mass transfer using a combined nonlinear membrane transport and film theory model, Desalination 109 (1997) 39–49.
[45] M.J. López-Mu~noza, A. Sottoa, J.M. Arsuagaa, B. Van der Bruggenb, Influence of membrane, solute and solution properties on the retention of phenolic compounds in aqueous solution by nanofiltration membranes, Sep. Purif. Technol 66 (2009) 194–201.
[46] J.W. Lee, T.O. Kwon, I.S. Moon, Performance of polyamide reverse osmosis membranes for steel wastewater reuse, Desalination 189 (2006) 309–322.